# Numerical Modelling of Pure Metal Solidification using OpenFOAM

Anup Singh, Alok Kumar, Arvind Kumar

# Numerical Modelling of Pure Metal Solidification using OpenFOAM

Anup Singh*, Alok Kumar, Arvind Kumar

Department of Mechanical Engineering
Indian Institute of Technology Kanpur, Kanpur - 208016, India
*singhanup2013031@gmail.com

**Abstract.** In this article, the isothermal phase change of pure metal is studied by using an opensource CFD tool. The single-domain mass, momentum and energy conservation equations are implemented in OpenFOAM to study the solidification behavior of the pure metal. The Darcy drag source term was used in momentum conservation equation for accounting the fluid flow in mushy region and enthalpy-porosity method was used to update the liquid fraction in each cell. The developed solver is well validated with the existing experimental results. The validated solver is used to simulate the isothermal phase change behavior of the pure tin (Sn). The results are presented for the evolution of flow field, temperature field and the solid/liquid interface. Results showed that the numerical simulation predictions are in good agreement with experimental measurements.

**Keywords:** Solidification, Pure metal, Numerical modelling and simulation, OpenFOAM.

## 1 Introduction

Solidification phenomena occurs in many engineering processes such as casting, welding, thermal spray coating, single crystal growth processes. The different solidification process parameters such as solidification rate, melt-front shape, and flow pattern in the liquid melt etc. affect the outcome of many manufacturing processes.

Solidification of pure metals is an isothermal phase change process where latent heat of fusion is released at the fusion temperature. During solidification of pure metals, the thermal convection currents are generated in the liquid region due to density variations caused by the temperature gradients present in the liquid. The presence of both solid and liquid phase during solidification of metals (see in fig.1) makes it very difficult to implement the governing equations in their classical form, as solid phase assumes a region of no flow and pure conduction mode of heat transfer whereas liquid phase assumes a region where classical form of momentum equation is applicable for fluid flow. Also, in the liquid region the heat transfer is governed by the conduction as well as convection.

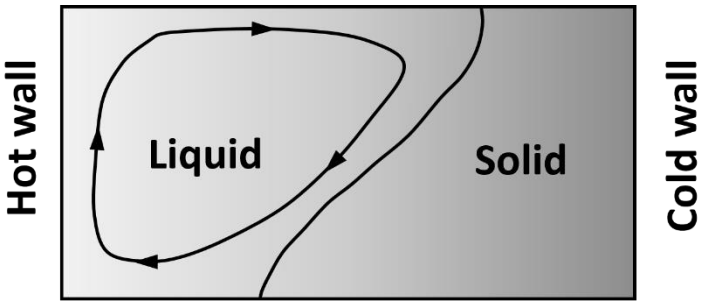


**Fig. 1.** Schematic diagram for Solidification of Pure Metals

Till date, numerous numerical investigations have been conducted to explore the flow-patterns due to the thermal convection during the solidification of pure metals. In the earlier numerical models, the different set of governing equation were used in the solid and liquid region to study the solidification behavior [1,7,9]. This type of modelling involves a moving interface which is managed by employing energy balance at the interface to keep track of the amount of energy released and solid-liquid interface. Later various other numerical methods like mixture model theory [2] and phase-averaged model [3] were developed for solving multiphase problems involving solid and liquid phase transition. In this type of modelling, a new source term is introduced for taking care of transformation of the classical form of governing equation from liquid to solid region and vice-versa. Generally, in case of momentum equation modelling, Carman-Kozney's equation (Darcy's law) [2] for flow through porous media is introduced as a source term for handling velocity jump across the solid-liquid interface. Whereas, in case of energy equation there are two methods for handling solid-liquid phase change which is Apparent heat capacity method [4] and Enthalpy-porosity method [5]. In Apparent heat capacity method, the specific heat capacity is modified by incorporating latent heat of fusion in heat capacity. Whereas in case of enthalpy porosity method a source term in accordance with enthalpy-porosity method is introduced in the energy equation. Subsequently, an enthalpy update scheme will be implemented in accordance to Chakroborty and Dutta [6] for updating the source term in the energy equation. In the past, most of the solidification simulations were carried out by either using some commercial simulation softwares or using commercial coding packages, all these are not available with open access.

In this paper, a 2D numerical model for the solidification of pure metal is developed in opensource CFD platform (OpenFOAM). The fixed-grid, single domain mixture models are used to study the phase change behavior of pure metal. The enthalpy-porosity method is used for handling the solid-liquid phase change in the energy equation. The numerical model is validated through experimental data reported by Wolff and Viskanta [7].

## 2 Model Description

The model presented in this paper was developed in OpenFOAM (opensource C++ based coding package) for understanding the flow dynamics in the liquid region during phase change. To simplify the model, following assumptions were made:

1. Incompressible, laminar and Newtonian flow in the liquid phase.
2. Constant physical properties of liquid and solid metal.
3. Boussinesq approximation for density variation of liquid metal with temperature.
4. The solid phase is assumed to be non-deforming and free of internal stress.

The computational domain for the present study is shown in figure 2. This computational domain replicates the experimental conditions used by Wolff and Viskanta [7] in their study of solidification of pure metal and the parameters used in the simulation like wall temperature and cavity dimensions are given in Table 1 [7].

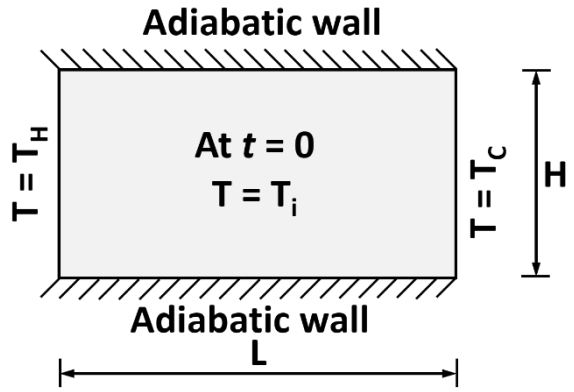


**Fig. 2.** Schematic diagram of Computational domain and boundary conditions

**Table 1.** Parameters for Simulation

| **Parameter** | **Value** |
|---|---|
| Hot Wall Temperature, $T_H$ (K) | 506.15 |
| Cold Wall Temperature, $T_C$ (K) | 502.15 |
| Initial Temperature, $T_{int}$ (K) | 506.15 |
| Height of Cavity ($H$) (cm) | 6.66 |
| Length of Cavity ($L$) (cm) | 8.89 |

## 2.1 Governing Equations

In the present study, the governing equations are defined using the fixed-grid continuum formulation with the single-domain approach. The continuum relations and the governing equations are written as follows.

***Continuum relations***

The continuum relations are defined as follows:

$$g_s + g_l = 1, \quad f_s + f_l = 1, \quad f_l = \frac{g_l \rho_l}{\rho}, \quad f_s = \frac{g_s \rho_s}{\rho}, \quad \rho = g_l \rho_l + g_s \rho_s \tag{1}$$

$$k = g_l\, k_l + g_s\, k_s, \qquad c_p = f_l c_{p_l} + f_s c_{p_s} \qquad \vec{u} = f_l \vec{u}_l + f_s \vec{u}_s \tag{2}$$

where $g$ is the volume fraction, $f$ is the mass fraction, $\rho$ is the mixture density, $k$ is the thermal conductivity, $\vec{u}$ is mixture velocity and $c_p$ is the specific heat. As volumetric shrinkage is neglected ($\rho_s = \rho_l$), the volume fraction $g$ and the mass fraction $f$ will be equivalent and interchangeable. In the continuum velocity ($\vec{u}$), the velocity of the solid phase is assumed stationary ($\vec{u_s} = 0$).

***Mass conservation***

The mass conservation equation is written as:

$$\nabla \cdot \vec{u} = 0 \tag{3}$$

***Momentum conservation***

The momentum conservation equation is given as:

$$\frac{\partial(\rho \vec{u})}{\partial t} + \vec{u} \cdot \nabla(\rho \vec{u}) = -\nabla p + \nabla \cdot (\mu \nabla \vec{u}) + A\vec{u} + \overrightarrow{S_b} \tag{4}$$

In the momentum equation the source term $A\vec{u}$ is introduced for handling sharp jump in velocity across solid-liquid interface. This source term is defined in such a way that it mimics the Carman – Kozeny equation for flow in a porous medium, and for cells undergoing phase change. It is defined as:

$$A\vec{u} = -\left[C \frac{(1 - f_l)^2}{{f_l}^3 - \epsilon}\right]\vec{u} \tag{5}$$

where, $C$ is a constant accounting for the mushy region morphology also known as mushy zone constant and $\epsilon$ is a small positive computational constant introduced to avoid division by zero.

Source term, $\overrightarrow{S_b}$ is for accounting the body force due to buoyancy and is implemented by using Boussinesq approximation.

$$\overrightarrow{S_b} = \rho \beta \vec{g}\left(T - T_{ref}\right) \tag{6}$$

where $\beta$ is thermal expansion coefficient. $T_{ref}$ is the reference temperature (Fusion temperature for pure metals).

***Energy conservation***

$$\frac{\partial(\rho C_P T)}{\partial t} + \vec{u} \cdot \nabla(\rho C_p T) = \nabla \cdot (K \nabla T) + S_h \tag{7}$$

The source term $S_h$ is defined as follows:

$$S_h = -\frac{\partial(\rho \Delta H)}{\partial t} \tag{8}$$

where ΔH is the Latent heat content of a cell.

***Enthalpy Update***

The enthalpy update scheme is implemented in accordance to Chakroborty and Dutta [6]. In case of pure metals, this update scheme takes the following form:

$$\left[\Delta H_p\right]_{n+1} = \left[\Delta H_p\right]_n + \frac{A_p}{A_p^0} \omega c_p \left[\left[T_p\right]_n - T_m\right] \tag{9}$$

where $[\Delta H_p]_{n+1}$ is updated nodal value of latent heat ,$[\Delta H_p]_n$ is current nodal value of latent heat, $[T_p]_n$ is current nodal value of temperature, $T_m$ is fusion temperature of metal and $\omega$ is relaxation factor.

After the computation of latent heat content of a cell, the liquid fraction, $f_l$ is computed as**:**

$$f_l = \frac{\Delta H}{L} \tag{10}$$

where $L$ is Latent heat of fusion.

It is possible that after the enthalpy update, some of the cells might result in non-physical value of $\Delta H$, i.e., values greater than $L$ or less than zero. To prevent $\Delta H$ from assuming non-physical values, the updated value of $\Delta H$ is needed to be bounded between 0 and $L$. This is achieved by implementing restriction as shown below:

$$[\Delta H_P]_{n+1} = \begin{matrix} 0 & \text{if } [\Delta H_P]_{n+1} < 0 \\ L & \text{if } [\Delta H_P]_{n+1} > L \end{matrix} \tag{11}$$

## 2.2 Numerical Implementation

The pisoFOAM solver from incompressible solver module was chosen as the base solver. The pisoFOAM solver was first modified for accounting buoyancy force term

in form of Boussinesq approximation [1-3] and energy conservation as described elsewhere [11]. Afterwards, Carman-Kozney's source term was added to the momentum equation and heat source term in accordance with enthalpy porosity method to energy equation. The heat source term was updated explicitly for every iteration using Eq. (9). The discretization of transient terms was carried out by first order forward Euler time marching scheme whereas discretization of convective terms was carried out by first order upwind scheme. For determining the optimal choice of grid distribution, a preliminary grid independence test was performed. This was done by plotting the temperature distribution along the central horizontal line ($y$ = 3.33 cm) in the computational domain (see in fig.3).

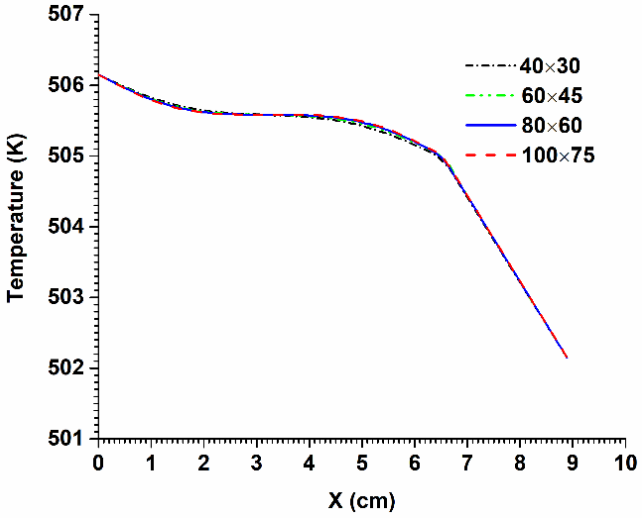


**Fig.3** Temperature Distribution for different grid distributions at $y$ = 3.33 cm

On the basis of grid independence test and computational cost, 80×60 grid sizes was selected based on the temperature distribution. A varying time step restricted by CFL criteria using was used during simulation (Co < 0.25). The isothermal phase change behaviour of the pure metal was studied by performing the simulations for the melting of pure tin (Sn). The thermophysical parameters for pure tin are given in Table 2 [10].

**Table 2** Thermophysical properties of Tin [10]

| **Thermo-physical Property** | **Value** |
|---|---|
| Density, $\rho$ (Kg m$^{-3}$) | 7500 |
| Freezing Temperature, $T_f$ (K) | 505 |
| Specific Heat Capacity, $C_P$ () | 200 |
| Thermal Conductivity, $k$ (W/mK) | 60 |
| Viscosity, $\mu$ (m$^2$/s) | $6\times10^{-3}$ |
| Latent Heat of Fusion, $L$ (J/Kg) | 60000 |
| Thermal Expansion Coefficient, $\beta$ (1/K) | $2.67\times10^{-4}$ |

## 3 Results and Discussion

The isothermal phase change behaviour of the pure metal was studied by performing the simulations for the melting of pure tin (Sn). The numerical model of isothermal phase change is validated against Experimental result. Figure 4 shows the validation of simulation results with the experimental results [7] of the solidification of pure tin. It is found that at the start, numerical model over predicts the solidification front but with time this discrepancy in the prediction of solidification front is reduced. There is still some difference in the simulated and experimental results which might be due to slight difference in the thermophysical properties used and deviation from the exact conditions used during experiment.

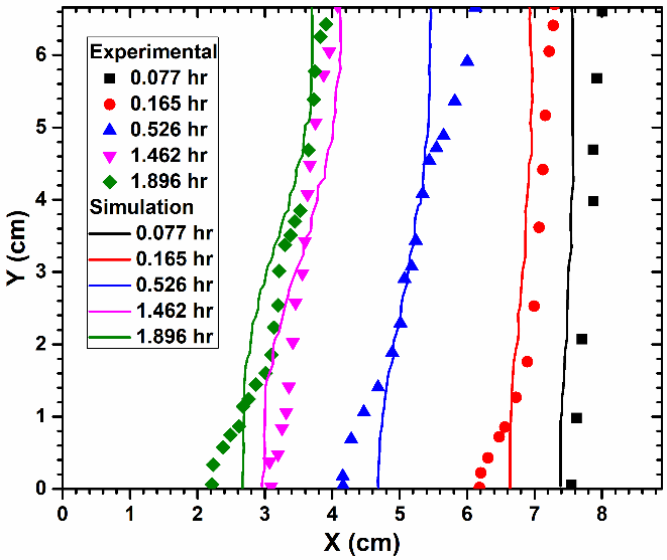


**Fig.4** Validation of Numerical Model with the experimental results of Wolff and Viskanta [7]

To further analyse the solver, the mean absolute percentage error (MAPE) between simulation and experimental results of the melt front locations is computed and tabulated in the Table 3. From Table 3, it can be seen that the MAPE lies below 10 % which is an acceptable limit for any solver predicting phase change in pure metals.

**Table 3** Computed Error for the performed simulation

| Mean Absolute Percentage Error [12] (MAPE in %) | | | | | |
|---|---|---|---|---|---|
| Time (hr) | 0.077 | 0.165 | 0.526 | 1.462 | 1.896 |
| MAPE | 0.97846 | 2.32802 | 4.38511 | 5.29687 | 6.0858 |

Figure 5 and 6 illustrate the evolution of velocity and temperature field during the solidification of pure tin. In figure 5 the velocity distribution in the liquid domain at different times is reported while the temperature profile for the same is reported in figure 6, from observing the figures it can be inferred that in the beginning (see figure corresponding to t = 100 second in Fig 5 and 6), solidification rate is quite high. This is mainly due to the large temperature difference existing at the beginning of process. Later the solidification rate slows down due to well established fluid flow and thermal field, until it falls down to zero due to system reaching a steady state.

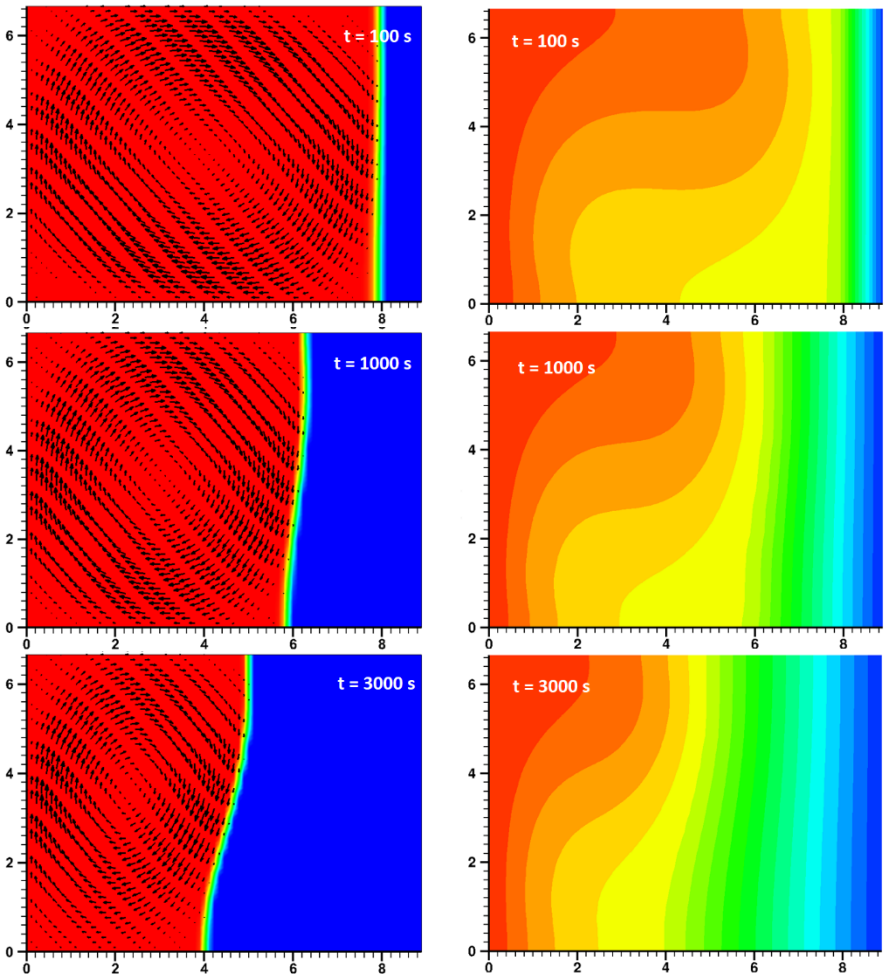

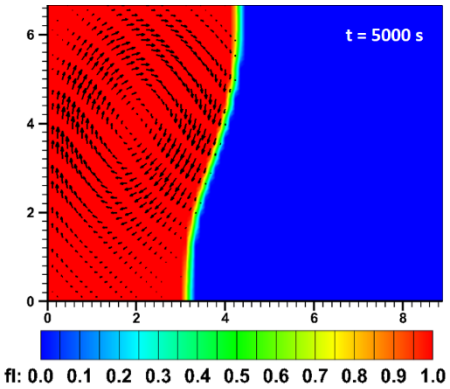


**Fig.5** Evolution of flow field in the liquid region during solidification of Tin

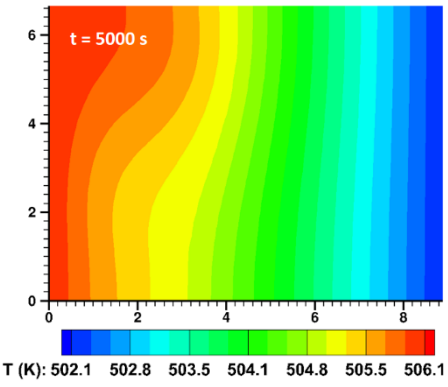


**Fig.6** Evolution of Temperature field in the Computational domain during solidification of Tin

The trend of decreasing solidification rate can also be inferred by observing the progress of melt front at various time steps. From figure 5, it is clear that the amount of tin solidified in the first 100 seconds is approximately half of the amount solidified in the next 900 seconds, and it keeps on taking more time to solidify further.

Figure 7 shows the variation of velocity magnitude along the central horizontal line ($y$ = 3.33 cm). In this figure the two peaks of velocity magnitude depict the two-velocity profile directed in the opposite direction of each other forming a loop which can be observed in the corresponding part in the figure 5. It can also be observed that the velocity becomes zero in the solidified region validating our assumption of mixture model theory. Furthermore, it is well established knowledge that in case of solidification inside an enclosed cavity the buoyant convection becomes the key factor in determining the shape of melt front and flow field in the liquid region. This behaviour of melt front is clearly captured in the shown figures. At the beginning the melt front assumes planer geometry but with time it adapts to the curvilinear geometry under the influence of buoyant convection.

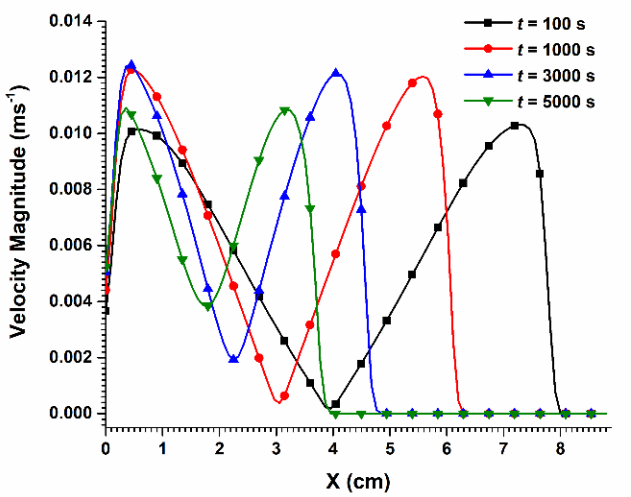


**Fig.6** Profile of Velocity Magnitude along central horizontal line (y = 3.33 cm)

## 4 Conclusion

From the above study, the following conclusions are drawn:

1. A reliable solver for the study of phase change in pure metals using OpenFOAM was developed. The developed solver was validated against the existing experimental results of the literature.
2. The developed model predicts the evolution of solidification front, velocity and temperature field for the solidification of pure metal.
3. From the validation study it is found that the simulation results are in good agreement with experimental results. Hence, the developed solver is capable of describing the solidification transport phenomena of the pure metals.
4. From the velocity vector plots, it was observed that the natural convection plays the key role in the growth of solidification interface of pure metals inside closed cavity.
5. The wavy interface was observed because of the flow field developed in the liquid region.

## References

1. Ho CJ, Viskanta R (1984) Heat transfer during melting from an isothermal vertical wall, Journal of heat transfer, vol 106(1), pp 12-19.
2. Bennon WD, Incropera FP (1987) A continuum model for momentum, heat and species transport in binary solid-liquid phase change systems—I. Model formulation, International Journal of Heat and Mass Transfer, vol 30(10), pp 2161-2170.
3. Jun N, Beckermann C (1991) A volume-averaged two-phase model for transport phenomena during solidification, Metallurgical Transactions B, vol 22(3), pp 349.

4. Voller VR (1997) An overview of numerical methods for solving phase change problems, Advances in numerical heat transfer, vol 1(9), pp 341-380.
5. Brent AD, Voller VR, Reid KTJ (1988) Enthalpy-porosity technique for modelling convection-diffusion phase change: application to the melting of a pure metal, Numerical Heat Transfer, Part A Applications, vol 13(3), pp 297-318.
6. Chakroborty S, Dutta P (2001) A generalized formulation for evaluation of latent heat functions in enthalpy-based macroscopic models for convection-diffusion phase change processes, Metallurgical and Materials Transactions B, vol 32(3), pp 562-564.
7. Wolff F, Viskanta R (1988) Solidification of a pure metal at a vertical wall in the presence of liquid superheat, International journal of heat and mass transfer, vol 31(8), pp 1735-1744.
8. Rady MA, Mohanty AK (1996) Natural convection during melting and solidification of pure metals in a cavity, Numerical Heat Transfer, Part A Applications, vol 29(1), pp 49-63.
9. Viskanta R (1988) Heat transfer during melting and solidification of metals, Journal of Heat Transfer, vol 110(4b), pp 1205-1219.
10. Alexiades V, Hannoun N, Mai TZ (2003) Tin melting: effect of grid size and scheme on the numerical solution, In Fifth Mississippi State Conference on Differential Equations and Computational Simulations, Electronic Journal of Differential Equations, vol 10, pp 55-69.
11. https://openfoamwiki.net/index.php/BuoyantBoussinesqPisoFoam
12. Mahato A, Kumar A (2016) Modeling transport phenomena of ice slurry in an ice forming unit, International Journal of Refrigeration, vol 69, pp 205-222.